

Synthesis and electrochemistry of ferrocenyldiazabutadiene metal carbonyl complexes (Fc-DAB)M(CO)₄ [M = Cr, Mo, W]

Benno Bildstein ^{a,*1}, Michael Malaun ^a, Holger Kopacka ^a, Marco Fontani ^b,
Piero Zanello ^{b,*2}

^a Institut für Allgemeine, Anorganische und Theoretische Chemie, Universität Innsbruck, Innrain 52a, A-6020 Innsbruck, Austria

^b Dipartimento di Chimica dell'Università di Siena, Via Aldo Moro, I-53100 Siena, Italy

Received 25 May 1999; accepted 30 July 1999

Abstract

The synthesis, characterization (UV–Vis, IR, MS, NMR), and electrochemistry (CV, DPV) of ferrocenyl diazabutadienes and their chromium, molybdenum, and tungsten tetracarbonyl complexes are reported in this study. The properties of these compounds are compared to those of *p*-methoxyphenyl diazabutadiene analogues, (a) allowing the clear distinction between ferrocene-based and diazabutadiene metal carbonyl localized redox processes in these multimetallic complexes, and (b) showing that the electronic interaction between the peripheral ferrocenyl substituents increases upon complexation to the Group 6 transition metal tetracarbonyl moieties. © 2000 Elsevier Science S.A. All rights reserved.

Keywords: Electrochemistry; Chromium complexes; Molybdenum complexes; Tungsten complexes; Ferrocene; Diimine ligands

1. Introduction

The coordination chemistry of 1,4-diaza-1,3-butadiene (R-DAB) ligands has attracted much interest due to their unusual electron donor and acceptor properties [1,2] and, more recently, due to their application in olefin homo- and co-polymerizations [3]. With the latter goal in mind we have been investigating the use of *N,N'*-diferrocenyldiazabutadiene (Fc-DAB; Fc = ferrocenyl) in nickel and palladium complexes as precatalysts for the cationic polymerization of olefins [4] with the intention to take advantage of the steric bulk of the *N*-ferrocenyl substituents in these complexes to suppress chain-termination processes. In addition, Fc-DAB has been proven to be the key starting material for the synthesis of *N,N'*-diferrocenyl-*N*-heterocyclic Wanzlick/Arduengo carbenes [5]. On the other hand, the presence of two redox-active ferrocenyl groups per DAB ligand results in conjugated oligometallic com-

pounds upon complexation with transition metal fragments. Therefore, it was of general interest to study the electronic influence of ferrocenyl substituents in these ligand systems and metal complexes. Here we report on the synthesis, properties and electrochemical behavior of metal carbonyl Fc-DAB complexes (Fc-DAB)M(CO)₄ with M = Cr, Mo, W, and the comparison of their properties with analogous *para*-methoxyphenyl-DAB [*p*-MeOC₆H₄-DAB] compounds. The *p*-methoxyphenyl moiety has been chosen as the most 'ferrocene-like' reference group because non-linear optical measurements [6] have shown comparable donor capacities for ferrocenyl and *p*-methoxyphenyl groups.

2. Results and discussion

2.1. Synthesis and characterization

Scheme 1 gives an overview of the compounds of this study. The ferrocenyl DAB ligands **1–3** have been prepared by condensation of glyoxal with the corresponding aminoferrocenes as was recently published [4].

¹*Corresponding author. Tel.: +43-512-507 5141; fax: +43-512-507 2934/2662; e-mail: benno.bildstein@uibk.ac.at

²*Corresponding author. Tel.: +43-512-507 5141; fax: +43-512-507 2934/2662; e-mail: zanello@unisi.it

Similarly, *p*-MeOC₆H₄-DAB (**4**), a known compound [7], was synthesized from *p*-anisidine and glyoxal. In contrast to **4** and other purely organic DAB ligands [1,2] which are yellow to orange compounds, the ferrocenyl DAB compounds **13** have an intense dark purple color (**1**: λ_{\max} = 524 nm, **2**: λ_{\max} = 537 nm [4,5]) indicating metal-to-ligand charge transfer (MLCT) which is to be expected for molecules incorporating redox-active ferrocenyl groups and a DAB backbone with two low-lying antibonding π^* orbitals [8]. In the following, only the DAB ligand **1** has been used for metal complex formation, because this ferrocenyl DAB compound is the most easily available and the 1'-ferrocenyl substituted ligands **2** and **3** have been synthesized mainly for increasing the steric bulk of the ligands [4].

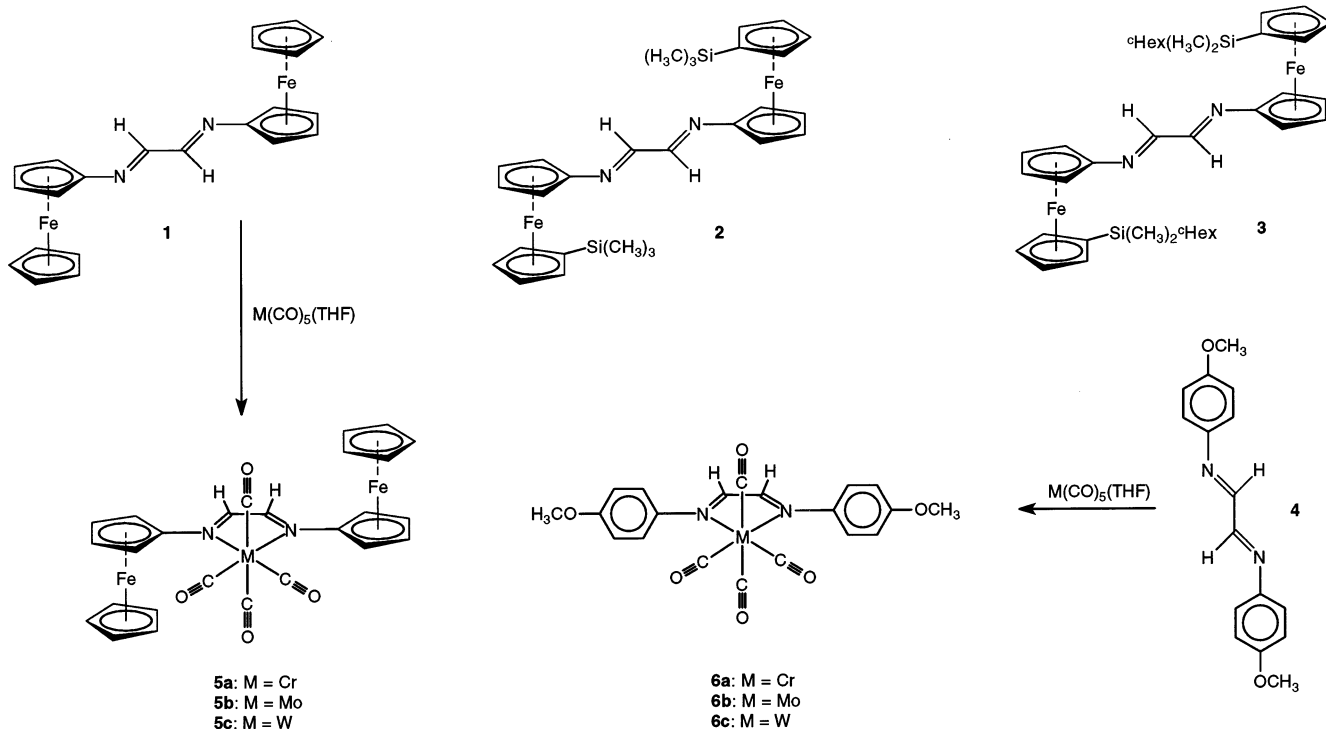
Reaction of **1** or **4** with photochemically generated substitution-labile M(CO)₅(THF) (M = Cr, Mo, W) yielded the corresponding heterometallic complexes (Fc-DAB)M(CO)₄ (**5a,b,c**) and (*p*-MeOC₆H₄-DAB)M(CO)₄ (**6a,b,c**), respectively, as dark green or blue air-stable compounds.

Fig. 1 shows a comparison of the UV–Vis spectra of all six metal carbonyl complexes. The compounds (*p*-MeOC₆H₄-DAB)M(CO)₄ (**6a,b,c**) have a moderately intense broad MLCT band centered at 600 nm (λ_{\max} (nm)/ ϵ : **6a**: 619/7000; **6b**: 593/10000; **6c**: 579/12000), characteristic for such (R-DAB)M(CO)₄ complexes with an organic R-DAB ligand, and which has been shown to consist of four separate electronic transitions [1,8]. In contrast, the complexes (Fc-DAB)M(CO)₄

(**5a,b,c**), show an additional long wavelength band (λ_{\max} (nm)/ ϵ : **5a**: 649/7000; **5b**: 581/12000, 702/11000; **5c**: 578/8400, 729/6300) clearly visible for **5b** and **5c** but unresolved in the case of **5a**. Obviously this additional MLCT transition is due to the presence of the *N*-ferrocenyl substituents, but a precise assignment cannot be given at this point.

The π -acceptor strength of the Fc-DAB ligand is slightly inferior to that of the *p*-MeOC₆H₄-DAB ligand, as evidenced by the IR ν_{C-O} frequencies of complexes **5a,b,c** in comparison to **6a,b,c** (see Section 4). Interestingly, the Fc-DAB complexes **5a,b,c** are much more soluble than the analogous *p*-MeOC₆H₄-DAB compounds **6a,b,c**, allowing full characterization by NMR spectroscopy in the case of the former, but preventing detection of the quaternary ¹³C NMR signals for **6b** and **6c**. In addition, the Fc-DAB complexes **5a,b,c** show the molecular ions in the FAB or EI mass spectra, respectively, in contrast to *p*-MeOC₆H₄-DAB compounds **6a,b,c**, which gave only low-mass fragment signals of no analytical value.

The ¹H and ¹³C NMR chemical shifts of the –N=CH–CH=N– subunit in the complexes **5a,b,c** and **6a,b,c** are slightly shielded/deshielded ($\delta(^1\text{H})$ **5a/5b/5c** = 8.47/8.43/8.81 ppm; $\delta(^1\text{H})$ **6a/6b/6c** = 8.31/8.38/8.68 ppm; $\delta(^{13}\text{C})$ **5a/5b/5c** = 154.3/152.6/154.4 ppm; $\delta(^{13}\text{C})$ **6a** = 158.2 ppm) in comparison to those of the free ligands Fc-DAB **1** and *p*-MeOC₆H₄-DAB **4** ($\delta(^1\text{H})$ **1/4** = 8.33/8.33 ppm; $\delta(^{13}\text{C})$ **1/4** = 157.8/157.3 ppm), similar to other (DAB)M(CO)₄ complexes [8].



Scheme 1. Overview of compounds **1**–**6** (°Hex = cyclohexyl).

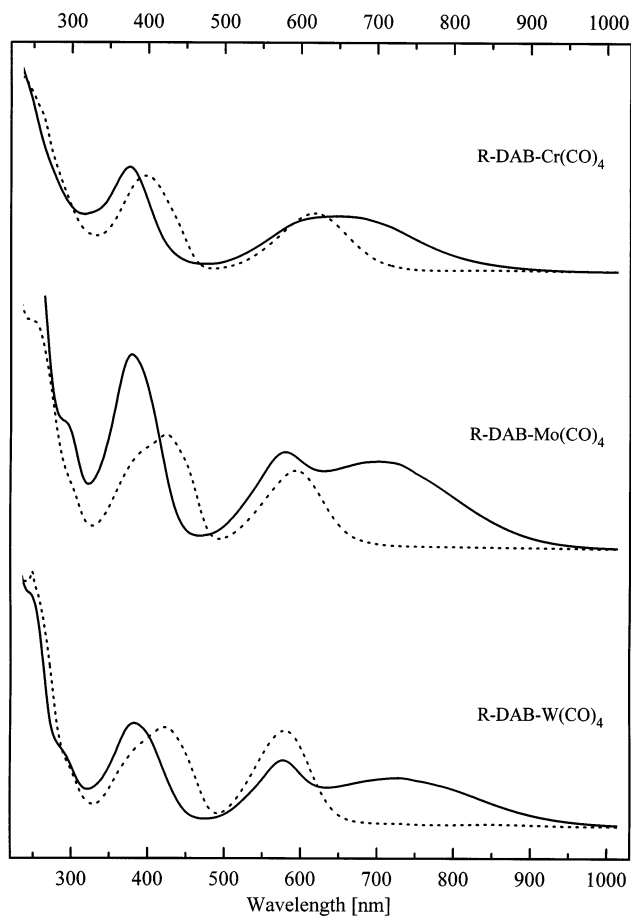


Fig. 1. Comparison of the UV-Vis spectra of R-DAB-M(CO)₄ compounds **5a,b,c** (R = Fc, —) and **6a,b,c** (R = *p*-MeOC₆H₄, ·····) in CH₂Cl₂ solution.

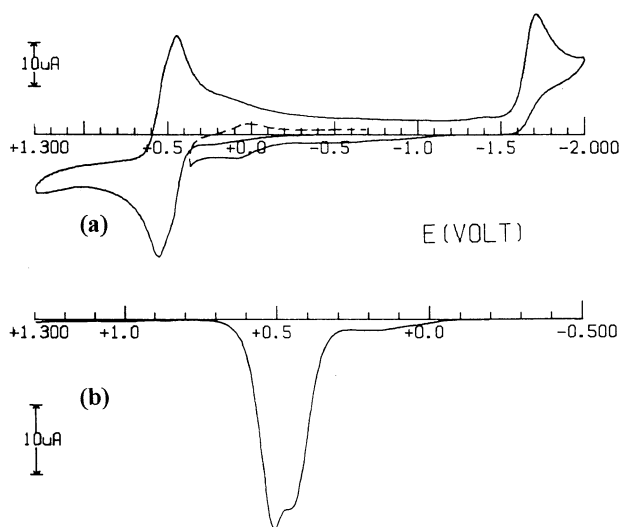


Fig. 2. Cyclic and differential pulse voltammograms of a CH₂Cl₂ solution containing Fc-DAB **1** (1.4 mmol l⁻¹) and NBu₄PF₆ (0.2 mol l⁻¹). Scan rates: cyclic voltammogram, 0.2 V s⁻¹; DPV, 0.004 V s⁻¹.

3. Electrochemistry

Fig. 2 illustrates the redox behavior of Fc-DAB **1** in dichloromethane solution either in cyclic or differential pulse voltammetry. It exhibits two essentially overlapped oxidations with features of chemical reversibility as well as an irreversible reduction. In agreement with the presence of two ferrocenyl subunits, controlled potential coulometry ($E_w = +0.8$ V) confirmed that the overall oxidation process consumes two electrons per molecule. Exhaustive oxidation made the original violet solution turn yellow–brown, but in spite of the apparent chemical reversibility of the oxidation process in the short times of cyclic voltammetry, a final cyclic voltammogram did not reveal any presence of Fc-DAB congeners. It is noteworthy that the sequential oxidations of the two ferrocenyl units occur at potential values differing by only 60 mV, whereas in Fc(CH=CH)₂Fc they are separated by about 130 mV [9]; the low conjugation operated by nitrogen atoms with respect to carbon atoms is hence reflected in a low, if any, electronic communication between the ferrocenyl units.

As far as the reduction step is concerned, in confirmation of the conceivable assignment to a diazabutadiene centered process, *p*-MeOC₆H₄-DAB (**4**) afforded a quite similar irreversible response. Based on the relative peak height, we assume that such reduction also involves a two-electron process. It seems interesting to point out that, as Fig. 2 shows, the backward profile after traversing the reduction step gives rise to a minor reversible peak-system at $E^{\circ} = +0.05$ V, which is just coincident with that of an authentic sample of ferrocenylamine, indicating partial chemical decomposition following the two electron addition.

A qualitatively similar behavior was displayed by the 1'-substituted ferrocenyl DAB compounds **2** and **3**, but in both cases the dication generated by macroelectrolysis appeared more stable as compared to **1**. In both cases the color of the solution turned from violet to green upon oxidation and displayed a broad UV-Vis band centered at about 600 nm, typical of ferrocenium species.

The formal electrode potentials of the redox changes exhibited by the DAB ligands **1–4** are summarized in Table 1. In spite of the fact that the trimethylsilyl substituents slightly increase the separation between the two sequential oxidations of the ferrocene units, a rough use of the K_{com} values could justify the assumption that in all cases the electrogenerable monocations are localized mixed-valent species.

More complicated appeared the voltammetric responses exhibited by the metallacomplexes (Fc-DAB)M(CO)₄ (**5a,b,c**) (M = Cr, Mo, W), but the availability of the related complexes (*p*-MeOC₆H₄-DAB)M(CO)₄ (**6a,b,c**) facilitated their interpretation. Fig. 3 shows the voltammetric profiles of (Fc-

Table 1
Formal electrode potentials (in V, vs. SCE) for the redox changes of DAB ligands **1**, **2**, **3**, **4** in CH₂Cl₂ solution

Compound	$E^\circ(2+/+)$ ^a	$E^\circ(+/0)$ ^a	ΔE°	K_{com}	$E_p(0/2-)$ ^b
1	+0.52	+0.46	0.06	10	-1.69
2	+0.54	+0.46	0.08	22	-1.73
3	+0.55	+0.46	0.09	33	-1.75
4	–	–	–	–	-1.67
Fe(C ₅ H ₅) ₂	–	+0.38	–	–	–

^a Peak potential value in DPV.

^b Measured at 0.2 V s⁻¹.

DAB)W(CO)₄ (**5c**) and its related complex (*p*-MeOC₆H₄-DAB)W(CO)₄ (**6c**). Apart from slight adsorption phenomena occurring in correspondence of the most anodic process (Fig. 3a), based on the voltammetric features of (*p*-MeOC₆H₄-DAB)W(CO)₄ (**6c**) it is quite clear that in the case of (Fc-DAB)W(CO)₄ (**5c**) the first irreversible oxidation at $E_p = 0.5$ V (accompanied by its backward peak at $E_p = -0.2$ V) and the reversible reduction process at $E_p = -1.0$ V have to be assigned to the redox processes of the metal fragment (DAB)W(CO)₄, which, if we assume that the reduction process at $E_p = -1.6$ V remains centered on the DAB fragment, should involve four- and two-electron transfers, respectively. Quite interestingly, the separation between the one-electron oxidations of the two ferrocenyl units of **5c** is significantly higher than in Fc-DAB **1** itself, i.e. 180 mV versus 60 mV, indicating that the formation of the W-DAB metallacycle notably increases the electronic communication between the peripheral ferrocene moieties. (Fc-DAB)Mo(CO)₄ (**5b**) gives rise to a voltammetric picture qualitatively similar to that of the tungsten analogue **5c**, but the separation between the two ferrocenyl-centred oxidations is slightly decreased to 140 mV.

Finally, as Fig. 4 illustrates, also (Fc-DAB)Cr(CO)₄ (**5a**) affords a response somewhat similar to that of (Fc-DAB)M(CO)₄ (**5b,c**) (M = Mo, W), even if the first (DAB)Cr(CO)₄-centred, (likely) two-electron oxidation is reversible, as was also observed for (*p*-MeOC₆H₄-DAB)Cr(CO)₄ (**6a**). However, it is interesting to note that the separation between the two sequential oxidations of the ferrocene groups further decreases to 120 mV, thus suggesting that the ability of the metallacycle (DAB)M(CO)₄ to favor the interaction between the two ferrocenyl donor units decreases according to the sequence: Cr < Mo < W. The same trend has been deduced from resonance Raman experiments of other (DAB)M(CO)₄ complexes [8]. All the pertinent electrochemical data are compiled in Table 2.

It has to be noted that the presence of the M(CO)₄ fragment exerts a significant electron-withdrawing effect on the Fc-DAB frame making the oxidation of the two ferrocenyl groups to shift toward more positive potential values by about 0.15–0.25 V. In addition,

based on the relevant K_{com} values, the mixed-valent Fe^{II}Fe^{III} species should become partially delocalized complexes.

4. Experimental

4.1. General

Reactions of air-sensitive materials were carried out using standard Schlenk techniques and vacuum-line

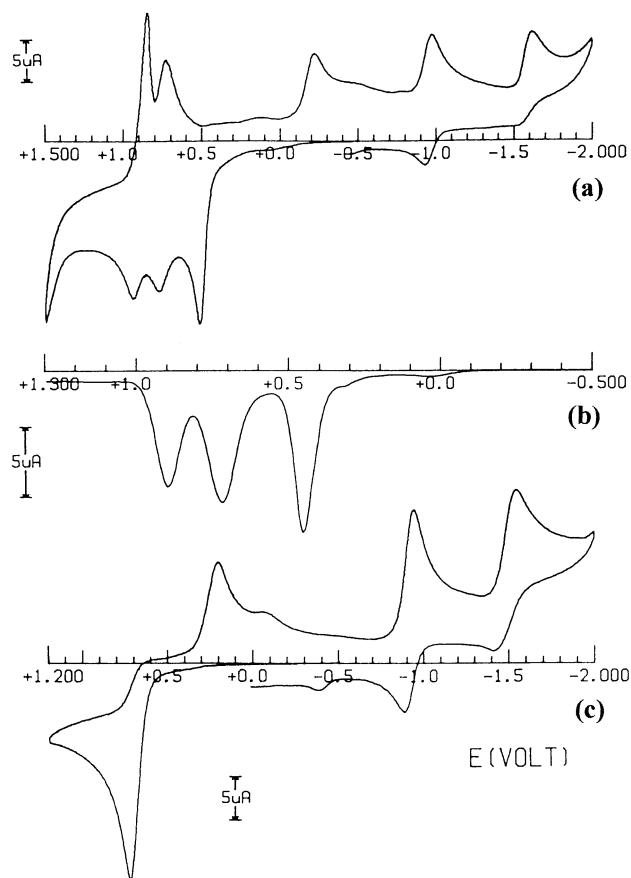


Fig. 3. Cyclic (a) and differential pulse (b) voltammograms of (Fc-DAB)W(CO)₄ (**5c**) (0.8 mmol l⁻¹); (c) cyclic voltammogram of (*p*-MeOC₆H₄-DAB)W(CO)₄ (**6c**) (0.9 mmol l⁻¹). CH₂Cl₂ solutions containing NBu₄PF₆ (0.2 mol l⁻¹) supporting electrolyte. Scan rates: cyclic voltammogram, 0.2 V s⁻¹; DPV, 0.004 V s⁻¹.

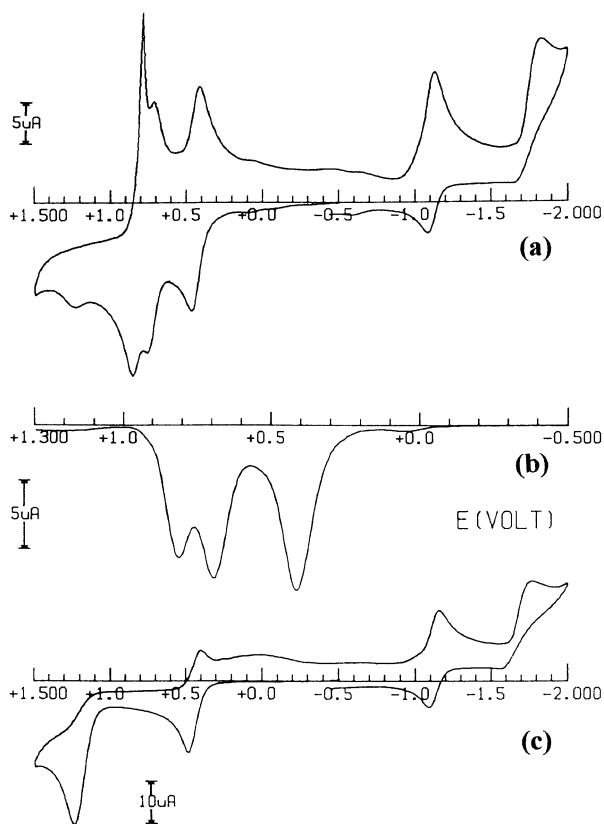


Fig. 4. Cyclic (a) and differential pulse (b) voltammograms of (Fc-DAB)Cr(CO)₄ (**5a**) (0.8 mmol l⁻¹); (c) cyclic voltammogram of (*p*-MeOC₆H₄-DAB)Cr(CO)₄ (**6a**) (1.1 mmol l⁻¹). CH₂Cl₂ solutions containing NBu₄PF₆ (0.2 mol l⁻¹) supporting electrolyte. Scan rates: cyclic voltammogram, 0.2 V s⁻¹; DPV, 0.004 V s⁻¹.

manipulations. Solvents were carefully deoxygenated, purified, and dried prior to use. Standard instrumentation and methods were as recently published [5]. The ferrocenyl DAB ligands **1–3** were synthesized by condensation of aqueous glyoxal with the corresponding aminoferrocenes [4,5]. *p*-Methoxyphenyl-DAB (**4**) was analogously prepared by condensation of glyoxal with *p*-anisidine and had spectral properties in concordance with published data [7].

Table 2
Comparison of the formal electrode potentials (V, vs. SCE; CH₂Cl₂ solution) for the redox changes of the (Fc-DAB)M(CO)₄ complexes **5a**, **5b**, **5c** and of the (*p*-MeOC₆H₄-DAB)M(CO)₄ complexes **6a**, **6b**, **6c**

Complex	Ferrocenyl oxidations			<i>K</i> _{com}	(DAB)M(CO) ₄ oxidation/reduction	
	<i>E</i> ^{o'} ₁ ^a	<i>E</i> ^{o'} ₂ ^a	Δ <i>E</i> ^{o'}		<i>E</i> ^{o'} _{ox}	<i>E</i> ^{o'} _{red}
5a	+0.70	+0.82	0.12	106	+0.44	-1.11
6a	–	–	–	–	+0.43	-1.12
5b	+0.61	+0.75	0.14	232	+0.54 ^b	-1.00
6b	–	–	–	–	+0.70 ^b	-1.12
5c	+0.72	+0.90	0.18	1100	+0.51 ^b	-0.96
6c	–	–	–	–	+0.73 ^b	-0.92

^a Peak potential value in DPV.

^b Peak potential value for irreversible processes (measured at 0.2 V s⁻¹).

4.2. Electrochemistry

Materials and apparatus for electrochemical measurements have been described elsewhere [10]. Differential pulse voltammograms were recorded under a pulse amplitude of 50 mV. All the potential values are referred to the saturated calomel electrode (SCE).

4.3. Synthesis of Fc-DAB-M(CO)₄ complexes (**5a**: M = Cr, **5b**: M = Mo, **5c**: M = W)

A THF solution of an excess of the corresponding metal hexacarbonyl M(CO)₆ (Cr: 0.6 g, 2.7 mmol; Mo: 1 g, 3.79 mmol; W: 0.823 g, 2.3 mmol) was photolyzed for 2 h with a 150 W high pressure mercury lamp. To the resulting solution of M(CO)₅(THF) was added a 15 ml THF solution of Fc-DAB **1** (Cr: 0.14 g, 0.33 mmol; Mo: 0.2 g, 0.47 mmol; W: 0.25 g, 0.59 mmol) and the mixture was stirred over night at ambient temperature, resulting in a blue–green solution. Work up: Solvent and volatile materials were removed in vacuo and the residue was chromatographed (Al₂O₃, ether/*n*-hexane) yielding a mixture of the product and the corresponding metal hexacarbonyl. Sublimation at reduced pressure removed the metal hexacarbonyl, yielding the pure product as a dark green powder (**5a**: 0.182 g, 0.31 mmol, 94%; **5b**: 0.238 g, 0.38 mmol, 80%; **5c**: 0.245 g, 0.34 mmol, 58%).

Data for **5a**: m.p. 180°C, dec. Anal. Found: C, 53.03; H, 3.44. Calc. for C₂₆H₂₀CrFe₂N₂O₄: C, 53.10; H, 3.43%. IR (KBr): cm⁻¹ 2004s (ν_{C=O}), 1910s (ν_{C=O}), 1885s (ν_{C=O}), 1823 (ν_{C=O}), 1636m, 1466m, 1437m, 1412w, 1261w, 1107m, 1053w, 1034w, 1003w, 821w, 652w, 619w, 540w, 522w, 490w, 474w. MS (FAB): *m/z*(%) 588(100) (M⁺). ¹H NMR (CDCl₃): δ 4.33 (s, 10H, Cp_{unsubst}), 4.52 (m, 4H, Cp_{subst}), 5.01 (m, 4H, Cp_{subst}), 8.47 (s, 2H, N=CHCH=N). ¹³C NMR (CDCl₃): δ 65.3 (Cp_{subst}), 69.2 (Cp_{subst}), 71.1 (Cp_{unsubst}), 90.7 (C(1) of Cp_{subst}), 154.3 (N=CH-CH=N). UV–Vis (CH₂Cl₂): λ_{max}(nm)/ε 376/13000, 649/7000. CV (CH₂Cl₂): -1.11, +0.44, +0.70, +0.82 V.

Data for **5b**: m.p. > 200°C, dec. *Anal.* Found: C, 49.23; H, 3.18. C₂₆H₂₀Fe₂MoN₂O₄. Calc.: C, 49.41; H, 3.19. IR (KBr): cm⁻¹ 2006s (ν_{C=O}), 1914s (ν_{C=O}), 1889s (ν_{C=O}), 1825 (ν_{C=O}), 1636m, 1557w, 1478s, 1431w, 1412w, 1107w, 1053w, 1034w, 1001w, 958w, 821w, 642w, 598w, 540w, 517w, 486m. MS (FAB): *m/z*(%) 632(60) (M⁺), 606(42) (M⁺ – CO), 578(37) (M⁺ – 2CO), 548(20) (M⁺ – 3CO), 520(100) (M⁺ – 4CO). ¹H NMR (CDCl₃): δ 4.34 (s, 10H, Cp_{unsubst}), 4.58 (m, 4H, Cp_{subst}), 5.07 (m, 4H, Cp_{subst}), 8.43 (s, 2H, N=CH–CH=N). ¹³C NMR (CDCl₃): δ 65.4 (Cp_{subst}), 70.01 (Cp_{subst}), 71.4 (Cp_{unsubst}), 90.0 (C(1) of Cp_{subst}), 152.6 (N=CH–CH=N). UV–Vis (CH₂Cl₂): λ_{max}(nm)/ε 379/24000, 581/12000, 702/11000. CV (CH₂Cl₂): –1.00, +0.54, +0.61, +0.75 V.

Data for **5c**: m.p. > 180°C, dec. *Anal.* Found: C, 43.25; H, 2.78. C₂₆H₂₀Fe₂N₂O₄W. Calc.: C, 43.37; H, 2.80. IR (KBr): cm⁻¹ 1998s (ν_{C=O}), 1885s (ν_{C=O}), 1823 (ν_{C=O}), 1472s, 1429m, 1246s, 1107m, 1036w, 1003w, 958w, 868w, 821s, 571w, 544w, 519w, 499w, 488w, 472w, 374m. MS (EI, 70 eV): *m/z*(%) 720(31) (M⁺), 606(100) (M⁺ – 4CO). ¹H NMR (CDCl₃): δ 4.34 (s, 10H, Cp_{unsubst}), 4.60 (m, 4H, Cp_{subst}), 5.10 (m, 4H, Cp_{subst}), 8.81 (s, 2H, N=CH–CH=N). ¹³C NMR (dmsod₆): δ 65.9 (Cp_{subst}), 69.8 (Cp_{subst}), 71.5 (Cp_{unsubst}), 154.41 (N=CH–CH=N). UV–Vis (CH₂Cl₂): λ_{max}(nm)/ε 383/13000, 578/8400, 729/6300. CV (CH₂Cl₂): –0.96, +0.51, +0.72, +0.90 V.

4.4. Synthesis of *p*-MeOC₆H₄-DAB-M(CO)₄ complexes (**6a**: M = Cr, **6b**: M = Mo, **6c**: M = W)

A THF solution of 1.5 mole equiv. of the corresponding metal hexacarbonyl M(CO)₆ (2.8 mmol; Cr: 0.615 g, Mo: 0.738 g, W: 0.983 g) was photolyzed for 2 h with a 150 W high pressure mercury lamp. To the resulting solution of M(CO)₅(THF) was added 0.5 g (1.9 mmol) *p*-An-DAB **4** and the mixture was stirred for 48 h at ambient temperature, resulting in a blue–purple solution. Work up: Solvent and volatile materials were removed in vacuo and the residue was chromatographed (Al₂O₃, ether/n-hexane) yielding a mixture of the product and the corresponding metal hexacarbonyl. Sublimation at reduced pressure removed the metal hexacarbonyl, yielding the pure product as a dark blue–purple powder (**6a**: 0.516 g, 1.2 mmol, 64%; **6b**: 0.648 g, 1.4 mmol, 73%; **6c**: 0.536 g, 1.0 mmol, 51%).

Data for **6a**: m.p. > 150°C, dec. *Anal.* Found: C, 55.40; H, 3.72. C₂₀H₁₆CrN₂O₆. Calc.: C, 55.56; H, 3.73. IR (KBr): cm⁻¹ 2932w, 2842w, 2014s (ν_{C=O}), 1943s (ν_{C=O}), 1883s (ν_{C=O}), 1809s (ν_{C=O}), 1601m, 1503s, 1476s, 1464m, 1443w, 1298w, 1252s, 1173m, 1026m, 835m, 684w, 652w, 617w, 544w. ¹H NMR (CD₂Cl₂): δ 3.88 (s, 6H, OCH₃), 7.01 (d, 4H, *J* = 9 Hz, C₆H₄), 7.42 (d, 4H, *J* = 9 Hz, C₆H₄), 8.31 (s, 2H, N=CH–CH=N). ¹³C

NMR (CD₂Cl₂): δ 56.0 (OCH₃), 114.4 (C₆H₄), 123.7 (C₆H₄), 158.2 (N=CH–CH=N). UV–Vis (CH₂Cl₂): λ_{max}(nm)/ε 396/12000, 619/7000. CV (CH₂Cl₂): –1.12, +0.43 V.

Data for **6b**: m.p. > 150°C, dec. *Anal.* Found: C, 50.28; H, 3.38. C₂₀H₁₆MoN₂O₆. Calc.: C, 50.43; H, 3.39. IR (KBr): cm⁻¹ 3015w, 2934w, 2842w, 2022s (ν_{C=O}), 1946s (ν_{C=O}), 1881s (ν_{C=O}), 1809s (ν_{C=O}), 1601m, 1505s, 1479m, 1464w, 1443w, 1298w, 1254s, 1173s, 1113w, 1026m, 835m, 557w, 540w. ¹H NMR (CD₂Cl₂): δ 3.88 (s, 6H, OCH₃), 7.01 (d, 4H, *J* = 9 Hz, C₆H₄), 7.54 (d, 4H, *J* = 9 Hz, C₆H₄), 8.38 (s, 2H, N=CH–CH=N). ¹³C NMR (CD₂Cl₂): δ not observed, overlapped by solvent peak: (OCH₃), 114.6 (C₆H₄), 124.1 (C₆H₄), not observed: (N=CH–CH=N). UV–Vis (CH₂Cl₂): λ_{max}(nm)/ε 425/14000, 593/10000. CV (CH₂Cl₂): –1.12, +0.70 V.

Data for **6c**: m.p. > 150°C, dec. *Anal.* Found: C, 42.46; H, 2.84. C₂₀H₁₆N₂O₆W. Calc.: C, 42.58; H, 2.86. IR (KBr): cm⁻¹ 3052w, 2981w, 2932w, 2842w, 2014s (ν_{C=O}), 1937s (ν_{C=O}), 1879s (ν_{C=O}), 1809s (ν_{C=O}), 1601m, 1505s, 1464s, 1443w, 1298m, 1254s, 1173m, 1113w, 1024m, 835m, 557w, 542w. ¹H NMR (CD₂Cl₂): δ 3.88 (s, 6H, OCH₃), 7.01 (d, 4H, *J* = 9 Hz, C₆H₄), 7.49 (d, 4H, *J* = 9 Hz, C₆H₄), 8.68 (s, 2H, N=CH–CH=N). ¹³C NMR (CD₂Cl₂): δ not observed, overlapped by solvent peak: (OCH₃), 114.5 (C₆H₄), 124.6 (C₆H₄), not observed: (N=CH–CH=N). UV–Vis (CH₂Cl₂): λ_{max}(nm)/ε 422/13000, 579/12000. CV (CH₂Cl₂): –0.92, +0.73 V.

Acknowledgements

B.B. acknowledges partial funding of this work by the European HCM-project ‘Electron and Energy Transfer in Model Systems and their Implications for Molecular Electronics’ (Grant No. CHRX-CT94-0538). P.Z. gratefully acknowledges the financial support of the University of Siena (ex quota 60%). We thank Professor Karl–Hans Ongania from the Institute of Organic Chemistry of the University of Innsbruck for measurement of FAB mass spectra.

References

- [1] G. van Koten, K. Vrieze, *Advan. Organometal. Chem.* 21 (1982) 151.
- [2] K. Vrieze, G. van Koten, in: G. Wilkinson, R.D. Gillard, J.A. McCleverty (Eds.), *Comprehensive Coordination Chemistry*, vol. 2, Pergamon, Oxford, 1987, p. 206.
- [3] L.K. Johnson, C.M. Moore, S.D. Arthur, J. Feldman, E.F. McCord, S.J. McLain, K.A. Kreutzer, M.A. Bennett, E.B. Coughlin, S.D. Ittel, A. Parthasarathy, D.J. Tempel, M. Brookhart, Patent WO 96/23010.
- [4] B. Bildstein, M. Malaun, A. Hradsky, A. Gonioukh, W. Micklitz, Patent pending DE 19920486.1 (1999).

- [5] B. Bildstein, M. Malaun, H. Kopacka, M. Mitterböck, K. Wurst, K.-H. Ongania, G. Opromolla, P. Zanello, *Organometallics* 18 (1999) 4325.
- [6] V. Alain, A. Fort, M. Barzoukas, C.-T. Chen, M. Blanchard-Desce, S.R. Marder, J.W. Perry, *Inorg. Chim. Acta* 242 (1996) 43.
- [7] J.M. Klerks, D.J. Stufkens, G. van Koten, K. Vrieze, *J. Organomet. Chem.* 181 (1979) 271.
- [8] L.H. Staal, D.J. Stufkens, A. Oskam, *Inorg. Chim. Acta* 26 (1978) 255.
- [9] A.-C. Ribou, J.-P. Launay, M.L. Sachtleben, H. Li, C.W. Spangler, *Inorg. Chem.* 36 (1996) 3735.
- [10] P. Zanello, F. Laschi, M. Fontani, C. Mealli, A. Ienco, K. Tang, X. Jin, L. Li, *J. Chem. Soc., Dalton Trans.* (1999) 965.